ACADEMIC PRESS

Available online at www.sciencedirect.com

SCIENCE DIRECT®

Journal of Magnetic Resonance 161 (2003) 132–137

JMR Journal of Magnetic Resonance

www.elsevier.com/locate/jmr

Pulse error compensating symmetric magic-echo trains

G.S. Boutis, P. Cappellaro, H. Cho, C. Ramanathan, and D.G. Cory*

Department of Nuclear Engineering, Massachusetts Institute of Technology, NW14-2217, 150 Albany Street, Cambridge, MA 02139, USA

Received 18 June 2002; revised 21 November 2002

Abstract

We present improved line-narrowing sequences for dipolar coupled spin systems, based on a train of magic-echoes which are compensated for the effects of finite pulse widths and utilize symmetry properties of supercycles. Sequences are introduced for spectroscopy and imaging by proper choice of a phase alternating scheme. Using a 16 pulse time-suspension magic-echo cycle, the highest level of line-narrowing achieved was 2.7 Hz for the [100] direction of a single crystal of calcium fluoride, a reduction in linewidth by 4 orders of magnitude.

PACS: 87.61.−c; 87.66.Uv; 61.18.Fs

Keywords: Magic-echo; Line narrowing; Finite pulse errors; Dipolar coupling; Time-reversal

1. Introduction

An appealing feature of average Hamiltonian theory is the ability to improve the line-narrowing efficiency of a multiple pulse cycle by constructing supercycles to compensate for any pulse errors and by designing symmetries into the toggling frame Hamiltonians. Such techniques have been known since the methods of coherent averaging were set forth by Haeberlen and Waugh [1]. An early example that demonstrated their potential was the introduction of the MREV8 pulse sequence [2,3] which corrected for the radiofrequency (RF) field inhomogeneity and finite pulse width effects that plagued the WAHUHA cycle [4]. In this paper we report on symmetric magic-echo (ME) pulse cycles which compensate for a variety of pulse errors. The TREV-8 sequence of Takegoshi and McDowell [5] and the TREV-16 sequence proposed by Matsui [6] are previously described examples of ME cycles. The efficiency of our improved ME cycle is demonstrated by line-narrowing the spectrum of a single crystal of calcium fluoride from 45 kHz to 2.7 Hz along the [100] direction.

The ME sequence is a multiple pulse cycle that refocuses the evolution of the dipolar interaction over a cycle, resulting in the formation of an echo [7]. In the language of average Hamiltonian theory, the cycle works since the form of the secular dipolar Hamiltonian in a toggling frame is scaled by a factor of $-1/2$, which evolves the system backward in time resulting in the formation of an echo.

A cycle of ME pulses may be designed to preserve the chemical shift Hamiltonian for use in spectroscopic studies, or by the virtual insertion of a π pulse, as a time-suspension sequence suppressing both chemical shift and dipolar Hamiltonians [8]. A characteristic feature of ME cycles is that sufficient line-narrowing may be achieved with long free evolution times (i.e., 10s of microseconds). This is in contrast to solid-echo based multiple pulse sequences where efficient line-narrowing is achieved only in the case where the free evolution times are made very short (typically less than 10 μs) [9]. This behavior may be understood by considering the convergence of the Magnus expansion [10]. For a train of ME pulses, convergence is readily met because high order terms are scaled by the inverse of the RF field strength which can be made much larger than the dipolar coupling and resonance offset, or any terms which are introduced due to pulse errors. In solid-echo based

* Corresponding author. Fax: 1-617-253-5405.
E-mail address: dcory@mit.edu (D.G. Cory).

1090-7807/03/$ - see front matter © 2003 Elsevier Science (USA). All rights reserved.
doi:10.1016/S1090-7807(03)00010-7

cycles though, these higher order terms (which are known to be strongly dependent on pulse errors such as finite pulse widths in the case of WAHUHA) are truncated only by making the time between pulses short.

From a technological point of view, the relatively long free-evolution times in a ME pulse sequence are appealing because pulsed gradients may be applied with ease for imaging or incoherent scattering experiments. Matsui et al. have used these methods and have achieved 50 μm resolution images of protonated solids [8,11–14]. Hepp and Miller [15] have incorporated the ME sequence with imaging techniques to map molecular orientations. In our investigations of spin diffusion rates in single crystals of calcium fluoride, we have used ME cycles with strong pulsed gradient fields to spatially encode a sinusoidal modulation of magnetization having a wavelength on the order of 100 nm [16]. The error correcting ME pulse cycles we report on here are shown to provide improved line-narrowing and are expected to be applicable to such investigations.

2. Theory

A ME train for time-reversing the evolution of a system of dipolar coupled spins is shown in Fig. 1. In the figure the free evolution time is denoted by $\tau - \alpha$, where 2α is the pulse width of the $\pi/2$ pulse. The toggling frame Hamiltonians at each point of the sequence were integrated over their respective intervals (δ_1–δ_6), and are given in Tables 1 and 2. The resulting zeroth order term of the chemical shift and dipolar Hamiltonian in the Magnus expansion are

$$\overline{H^0_{\Delta\omega}} = \frac{1}{3\tau}\frac{\Delta\omega}{\omega_{\mathrm{RF}}} I_y[1-\cos\omega_{\mathrm{RF}}(2\tau-\alpha)] - \frac{1}{3\tau}\frac{\Delta\omega}{\omega_{\mathrm{RF}}} I_x\left[\sin\omega_{\mathrm{RF}}(2\tau-\alpha)+\frac{4}{\pi}\omega_{\mathrm{RF}}\alpha\right], \quad (1)$$

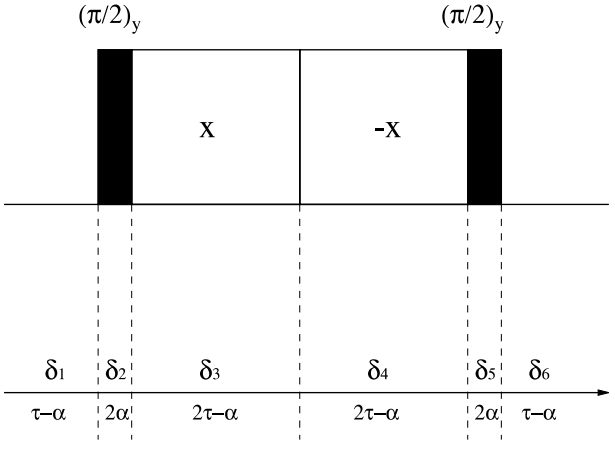

Fig. 1. The ME sequence for time-reversing the evolution of a system of nuclear-spins coupled by a dipolar interaction [7]. The duration of the $\pi/2$ pulses is 2α.

$$\overline{H^0_{\mathrm{D}}} = \omega_{\mathrm{D}} I_z I_z - \omega_{\mathrm{D}}\mathbf{I}\cdot\mathbf{I} + \frac{1}{4\tau}\frac{\omega_{\mathrm{D}}}{\omega_{\mathrm{RF}}} I_x I_x[2\omega_{\mathrm{RF}}(2\tau+\alpha) + \sin 2\omega_{\mathrm{RF}}(2\tau-\alpha)] + \frac{1}{4\tau}\frac{\omega_{\mathrm{D}}}{\omega_{\mathrm{RF}}} I_y I_y[2\omega_{\mathrm{RF}}(2\tau-\alpha) - \sin 2\omega_{\mathrm{RF}}(2\tau-\alpha)] - \frac{1}{2\tau}\frac{\omega_{\mathrm{D}}}{\omega_{\mathrm{RF}}}[I_x I_y + I_y I_x]\sin^2 \times \omega_{\mathrm{RF}}(2\tau-\alpha), \quad (2)$$

where ω_{D} is the dipolar coupling constant, ω_{RF} is the RF field strength, and $\Delta\omega$ is the resonance offset.

In the ideal case of δ-function $\pi/2$ pulses (i.e., $\alpha \to 0$), the zeroth order dipolar and offset terms of the Magnus expansion are both zero when $\omega_{\mathrm{RF}}\tau = n\pi$, $n \in Z$. However, the normal approach to reducing these terms is by application of high RF field strengths. Under the readily achievable experimental conditions of $\omega_{\mathrm{D}}/\omega_{\mathrm{RF}} \ll 1$, $\Delta\omega/\omega_{\mathrm{RF}} \ll 1$, and $\omega_{\mathrm{RF}}\tau \gg 1$, the zeroth order terms of the Magnus expansion are still close to zero.

By changing the last $\pi/2$ pulse in Fig. 1 to $\bar{y}$, the ME sequence may time-reverse the dipolar evolution of the spin system, but does not remove the chemical shift Hamiltonian making it applicable for spectroscopic studies. In either case of a time-suspension or spectroscopic sequence, the ME cycle is sensitive to pulse errors such as phase transients, finite pulse width effects and other pulse errors. In addition, the higher order cross-terms of the Magnus expansion may be nonzero but may be easily accounted for by considering the symmetry properties of the cycle.

In a symmetric cycle, where the toggling frame Hamiltonians indicated by $\widetilde{H}(t)$ have the property $\widetilde{H}_{\mathrm{int}}(t) = \widetilde{H}_{\mathrm{int}}(t_{\mathrm{c}} - t)$ over a cycle time t_{c}, all the odd order terms of the Magnus expansion are zero [9,17]. Referring to Tables 1 and 2, there is a change in sign in the $I_xI_z + I_zI_x$ terms of the toggling frame Hamiltonians during the finite $\pi/2$ pulses, and in the $I_xI_y + I_yI_x$ terms during δ_3 and δ_4. Consequently, the ME sequence in Fig. 1 is not symmetric. In the following we show how symmetric cycles may be constructed to remove the dipolar, offset, first order dipolar-offset cross term and all odd order terms of the Magnus expansion, while accounting for pulse errors, transients, and finite pulse width effects. The design of cycles from the basic single ME pulse sequence of Fig. 1 follows below for both time-suspension and spectroscopic sequences.

A four pulse phase alternating ME sequence, hereafter referred to as SME4, that is symmetric in the toggling frame dipolar and offset Hamiltonians for δ-function $\pi/2$ pulses is shown in Fig. 2. The symmetry condition results when $2\omega_{\mathrm{RF}}\tau = (2n+1)\pi$, $n \in Z$. The extent to which this condition may be met is discussed in the next section. It should be noted that with this phase alternating scheme the SME4 sequence is robust against symmetric phase transients and also compensates for errors in the $\pi/2$ pulses. An additional feature of the

Table 1
Toggling frame dipolar Hamiltonians and effective toggling frame dipolar Hamiltonians for the sequence shown in Fig. 1

Time	Toggling frame dipolar Hamiltonian	Integrated dipolar Hamiltonian
δ_1	$\omega_D(3I_zI_z - \mathbf{I}\cdot\mathbf{I})$	$\omega_D\frac{(\tau-\alpha)}{6\tau}(3I_zI_z - \mathbf{I}\cdot\mathbf{I})$
δ_2	$3\omega_D[I_zI_z\cos^2\omega_{RF}t + I_xI_x\sin^2\omega_{RF}t]$ $-\frac{3}{2}\omega_D(I_xI_z + I_zI_x)\sin 2\omega_{RF}t - \omega_D\mathbf{I}\cdot\mathbf{I}$	$\frac{1}{2\tau}\frac{\omega_D}{\omega_{RF}}[\omega_{RF}\alpha(I_xI_x + I_zI_z) - \frac{1}{2}(I_xI_z + I_zI_x)] - \frac{1}{3\tau}\omega_D\alpha\mathbf{I}\cdot\mathbf{I}$
δ_3	$3\omega_DI_xI_x\cos^2\omega_{RF}t + 3\omega_DI_yI_y\sin^2\omega_{RF}t$ $-\frac{3}{2}\omega_D(I_xI_y + I_yI_x)\sin 2\omega_{RF}t - \omega_D\mathbf{I}\cdot\mathbf{I}$	$\frac{1}{8\tau}\frac{\omega_D}{\omega_{RF}}I_xI_x[2\omega_{RF}\xi + \sin 2\omega_{RF}\xi]$ $+\frac{1}{8\tau}\frac{\omega_D}{\omega_{RF}}I_yI_y[2\omega_{RF}\xi - \sin 2\omega_{RF}\xi]$ $-\frac{1}{4\tau}\frac{\omega_D}{\omega_{RF}}(I_xI_y + I_yI_x)\sin^2\omega_{RF}\xi - \omega_D\frac{2\tau-\alpha}{6\tau}\mathbf{I}\cdot\mathbf{I}$
δ_4	$3\omega_DI_xI_x\cos^2\omega_{RF}(t-\xi) + 3\omega_DI_yI_y\sin^2\omega_{RF}(t-\xi)$ $+\frac{3}{2}\omega_D(I_xI_y + I_yI_x)\sin 2\omega_{RF}(t-\xi) - \omega_D\mathbf{I}\cdot\mathbf{I}$	$\frac{1}{8\tau}\frac{\omega_D}{\omega_{RF}}I_xI_x[2\omega_{RF}\xi + \sin 2\omega_{RF}\xi] + \frac{1}{8\tau}\frac{\omega_D}{\omega_{RF}}I_yI_y$ $[2\omega_{RF}\xi - \sin 2\omega_{RF}\xi] - \frac{1}{4\tau}\frac{\omega_D}{\omega_{RF}}(I_xI_y + I_yI_x)\sin^2$ $\omega_{RF}\xi - \omega_D\frac{2\tau-\alpha}{6\tau}\mathbf{I}\cdot\mathbf{I}$
δ_5	$3\omega_D[I_zI_z\cos^2\omega_{RF}t + I_xI_x\sin^2\omega_{RF}t]$ $+\frac{3}{2}\omega_D(I_xI_z + I_zI_x)\sin 2\omega_{RF}t - \omega_D\mathbf{I}\cdot\mathbf{I}$	$\frac{1}{2\tau}\frac{\omega_D}{\omega_{RF}}[\omega_{RF}\alpha(I_xI_x + I_zI_z) + \frac{1}{2}(I_xI_z + I_zI_x)] - \frac{1}{3\tau}\omega_D\alpha\mathbf{I}\cdot\mathbf{I}$
δ_6	$\omega_D(3I_zI_z - \mathbf{I}\cdot\mathbf{I})$	$\omega_D\frac{(\tau-\alpha)}{6\tau}(3I_zI_z - \mathbf{I}\cdot\mathbf{I})$

ω_D is the dipolar frequency, $2\omega_{RF}\alpha = \frac{\pi}{2}$, where 2α is the pulse length, and $\xi = 2\tau - \alpha$.

Table 2
Toggling frame chemical shift Hamiltonians and Effective toggling frame chemical shift Hamiltonians for the sequence shown in Fig. 1

Time	Toggling frame offset Hamiltonian	Integrated offset Hamiltonian
δ_1	$\Delta\omega I_z$	$\Delta\omega\frac{(\tau-\alpha)}{6\tau}I_z$
δ_2	$\Delta\omega[I_z\cos\omega_{RF}t - I_x\sin\omega_{RF}t]$	$\frac{1}{6\tau}\frac{\Delta\omega}{\omega_{RF}}(I_z - I_x) = \Delta\omega\frac{2\alpha}{3\tau\pi}(I_z - I_x)$
δ_3	$\Delta\omega[-I_x\cos\omega_{RF}t + I_y\sin\omega_{RF}t]$	$\frac{1}{6\tau}\frac{\Delta\omega}{\omega_{RF}}I_y[1 - \cos\omega_{RF}\xi] - \frac{1}{6\tau}\frac{\Delta\omega}{\omega_{RF}}I_x\sin\omega_{RF}\xi$
δ_4	$\Delta\omega[-I_x\cos\omega_{RF}(t-\xi) + I_y\sin\omega_{RF}(t-\xi)]$	$\frac{1}{6\tau}\frac{\Delta\omega}{\omega_{RF}}I_y[1 - \cos\omega_{RF}\xi] - \frac{1}{6\tau}\frac{\Delta\omega}{\omega_{RF}}I_x\sin\omega_{RF}\xi$
δ_5	$\Delta\omega[-I_z\cos\omega_{RF}t - I_x\sin\omega_{RF}t]$	$\frac{1}{6\tau}\frac{\Delta\omega}{\omega_{RF}}(-I_z - I_x) = \Delta\omega\frac{2\alpha}{3\tau\pi}(-I_z - I_x)$
δ_6	$-\Delta\omega I_z$	$-\Delta\omega\frac{(\tau-\alpha)}{6\tau}I_z$

$\Delta\omega$ refers to the offset frequency, $2\omega_{RF}\alpha = \frac{\pi}{2}$, where 2α is the pulse length, and $\xi = 2\tau - \alpha$.

SME4 cycle is that it removes the effect of finite pulse width errors on $\overline{H^0_{\Delta\omega}}$, but not on $\overline{H^0_D}$.

The sequence shown in Fig. 1 also performs a π inversion on the bulk magnetization. When several ME cycles are combined back-to-back, the error in the π inversion may accumulate, resulting in an unwanted evolution. Phase alternating techniques well-known in heteronuclear decoupling investigations may be applied with this cycle to correct for these errors [22–26]. The well-known MLEV4 cycle $RR\overline{RR}$ (where R indicates a π rotation) may be permuted to $R\overline{RR}R$, resembling the SME4 cycle in Fig. 2. To some extent the SME4 cycle removes the effects of pulse errors, and may be combined with higher order cycles to remove the residual rotation due to errors. Levitt et al. have shown that the residual rotation of $R\overline{RR}R$ may be accounted for by combining $RR\overline{RR}$ to this cycle yielding the MLEV8 pulse sequence, $R\overline{RR}RRR\overline{RR}$. The higher order MLEV sequences MLEV16, MLEV32, MLEV64 have been shown to compensate for the residual rotations introduced in each subcycle and may also be combined with the SME4 sequence. The introduction of each supercycle; however, destroys the symmetry property of the SME4 sequence, but corrects for residual rotations introduced due to pulse errors. This procedure generates the family of pulse sequences designated by $SME4_x$.

In order to compensate for the effects of finite pulse width errors on $\overline{H^0_D}$ in the SME4 sequence, an additional phase alternation is necessary. The idea is to remove an unwanted Hamiltonian in a portion of a cycle by introducing the same Hamiltonian with opposite sign in another portion by proper phase alternation of the pulses. These methods have been demonstrated to be very useful in multiple pulse sequences based on solid-echoes [2,3,18]. A phase alternating sequence which is composed of four SME4 cycles, hereafter referred to as SME16, that removes the effects of finite pulse widths on $\overline{H^0_D}$ is shown in the lower portion of Fig. 2. The finite pulse width contribution of the first four pulses to $\overline{H^0_D}$ is $(\omega_D\alpha/6\tau)[I_xI_x - I_yI_y]$, the second set of four pulses contributes an amount $-(\omega_D\alpha/6\tau)[I_xI_x - I_yI_y]$, cancelling that of the first four pulses of the cycle. Finite pulse width errors on $\overline{H^0_D}$ are therefore completely removed over half of the SME16 cycle. In order to symmetrize the sequence the half-cycle is repeated in reverse. As in the SME4 sequence, symmetry results when $2\omega_{RF}\tau = (2n+1)\pi$, $n \in Z$. Under these conditions the first order

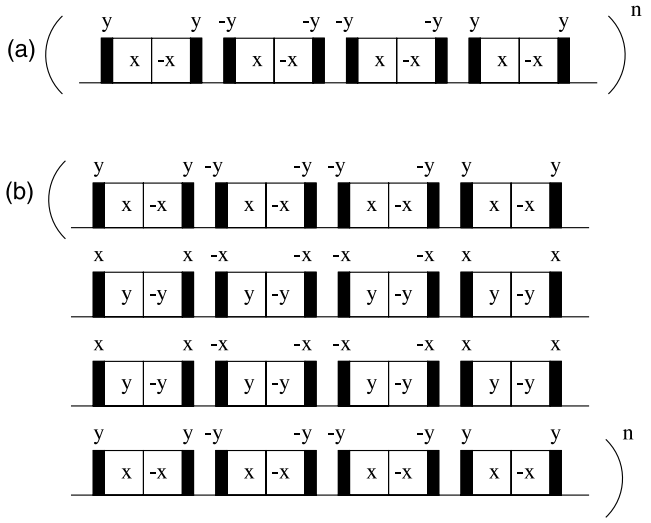

Fig. 2. (a) (SME4) A phase alternated ME sequence that makes the offset and dipolar toggling frame Hamiltonians symmetric over the cycle for δ-function $\pi/2$ pulses and is robust against symmetric phase transients and pulse errors. (b) (SME16) A ME train with the same features as the sequence above it, except that the effects of finite pulse widths on $\overline{H_{\mathrm{D}}^{0}}$ and $\overline{H_{\Delta\omega}^{0}}$ are completely removed.

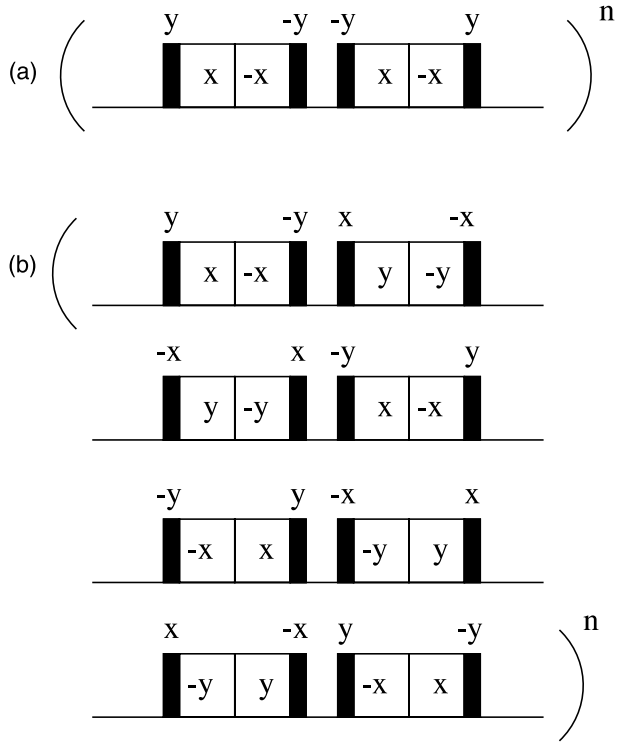

Fig. 3. (a) (SME2/TREV-8)A phase alternating ME sequence that makes the toggling frame dipolar Hamiltonian symmetric over the cycle for δ-function $\pi/2$ pulses. (b) (SME8) A sequence with the same features as the one above it but is also symmetric in the toggling frame dipolar and offset Hamiltonians including the effects of finite pulse widths. In both the sequences the offset Hamiltonians linear in I_z are not removed during the free evolution times, making the cycles applicable for spectroscopic studies.

dipolar-offset cross-term and all odd order-terms of the Magnus expansion are zero for both sequences in Fig. 2.

A symmetric sequence applicable for spectroscopic studies, referred to as SME2 in the rest of this paper, is shown in Fig. 3, and is identical to the TREV-8 sequence [5]. The SME2 sequence is also symmetric when $2\omega_{\mathrm{RF}}\tau = (2n+1)\pi$, $n \in Z$. An additional feature of the cycle is that it removes the effects of Hamiltonians linear in I_z during the spin locking fields of the ME pulse, independent of the value of $\omega_{\mathrm{RF}}\tau$. The SME2 sequence may also be combined with a similar phase alternating scheme discussed above for the SME16 cycle to compensate for the effects of finite pulse widths on $\overline{H_{\mathrm{D}}^{0}}$. The SME8 sequence shown in Fig. 3 compensates for finite pulse width errors in $\overline{H_{\mathrm{D}}^{0}}$ and has the same properties as the SME2 sequence.

3. Experiments and discussion

The experiments were performed at 2.35 T (100.15 MHz ^{1}H, 94.2 MHz ^{19}F) on a Bruker Avance spectrometer using a home built probe. The RF coil geometry used has been shown to provide homogeneous fields over a small sample volume [21]. All of the experiments were conducted on resonance, and the sample size was approximately 1 mm^3.

We tested the symmetric, error compensating sequences shown in Figs. 2 and 3 on a single crystal of calcium fluoride aligned approximately along the [100] direction. The line-narrowing efficiency in Hertz of each cycle as a function of τ is given in Table 3. The linewidths reported are the measured full-width at half maximum (FWHM) of the Fourier transformed data. The natural linewidth was measured to be approximately 45 kHz (this is actually the width across the Pake doublet). The spectrometer was tuned by using the procedure suggested by Burum et al. [19,20].

For the symmetric ME pulse sequence, SME4, the experimental data indicate that the higher order family of MLEV error compensating sequences (SME4$_x$) improved the line-narrowing for a given τ spacing, but the variation as a function of τ for each sequence changed. A possible cause of this variation is that the symmetry of the cycle is destroyed by introducing the MLEV supercycles.

The TREV16 cycle introduced by Matsui [6] is a four pulse ME sequence which is symmetric in the dipolar and offset toggling frame Hamiltonians for δ-function $\pi/2$ pulses. Both the TREV16 pulse sequence and the SME4 sequence of Fig. 2 appear to provide relatively the same line-narrowing for long τ spacings. The TREV16 cycle did not work well for very short τ spacings ($\sim$10 μs). A possible source of this behavior is the unaccounted for finite pulse width effects. The SME4 sequence shown in Fig. 2 did not work for τ spacings less

Table 3
Experimental data for each ME pulse cycle discussed in the text with measured linewidth given as a function of τ in units of Hz, tested on single crystal calcium fluoride along the [100] direction

Pulse sequence	10 μs	15 μs	20 μs	30 μs	40 μs	50 μs
TREV16 [6]	199	176	150	122	109	108
SME4	—	—	100	111	95	112
$SME4_8$	—	—	80	81	91	105
$SME4_{16}$	—	—	70	68	96	112
$SME4_{32}$	—	—	60	69	96	108
$SME4_{64}$	—	—	**55**	**71**	**94**	**96**
SME16	**2.7**	**33**	67	93	105	122
SME8	113	90	76	92	111	150
SME2/TREV-8	—	—	375	388	350	345
MSHOT3 [28]	152	170	160	187	219	211

The symmetric four pulse cycle shown in the top of Fig. 2 was applied with the particular family of MLEV supercycle indicated in the table by $SME4_x$. For short τ spacings these cycles resulted in a spin-locking field (see text). The 16 pulse symmetric ME train, SME16, provided very efficient line narrowing for short τ spacings but did not work well for longer τ spacings. The best line-narrowing achieved at each value of τ is indicated in bold. For a crystal oriented along the [111] direction each of the sequences demonstrated improved line-narrowing.

than 30 μs because a spin-locking field resulted. Spin-locking effects with the ME train have been discussed by Matsui [6,27].

We found that the SME16 cycle, shown in Fig. 2, provided efficient line-narrowing for short τ spacings. Experimental data indicating the capabilities of this sequence is shown in the Fig. 4. The data show an oscillation which is induced intentionally by introducing a phase shift on one of the pulses in the cycle to produce an effective ϕI_z Hamiltonian, demonstrating that the spins are not spin-locked. The data in Fig. 4 were acquired stroboscopically with a τ spacing of 10 μs, a cycle time of 960 μs ($= 96\tau$), and a 1.5 μs $\pi/2$ pulse. The line-narrowing with this cycle was measured to be approximately 27 Hz with the phase shift, and was found to be even smaller without the phase shift (2.7 Hz)—the FID is shown in the inset of Fig. 4. A similar measurement along the [111] direction of the crystal resulted in a linewidth of 0.5 Hz.

Recently, Howhy and Nielsen suggested using z-rotational decoupling (a form of second averaging) to improve the line-narrowing properties of the magic echo train [28]. Table 2 also shows the results obtained for their MSHOT3 sequence. We did not investigate higher order MSHOT sequences.

The efficiency of the SME16 sequence may be taken advantage of in applications of solid state imaging or in NMR scattering experiments by applying a short gradient pulse during the free evolution times. The generation of short, intense gradient pulses (on the order of 6 μs) has been developed by Conradi et. al [29] and been applied in multiple pulse sequences constructed from solid echoes for imaging solids [30].

The sequences which resolve the chemical shift Hamiltonian, SME2 and SME8, provided more efficient line narrowing than a sequence where no phase alternation is applied. As was the case for the SME4 cycle, the SME2 cycle also resulted in a locking field for very

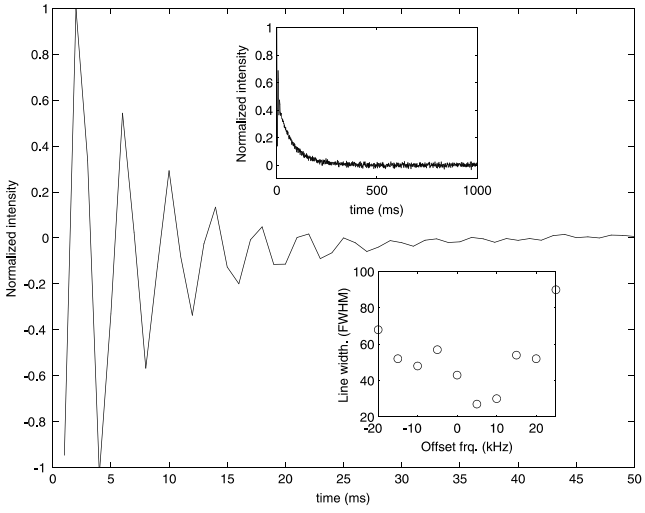

Fig. 4. Experimental data from a stroboscopic detection of the SME16 cycle applied on single crystal calcium fluoride aligned approximately along the [100] direction. An artificial I_z rotation was induced by phase shifting one of the ME pulse to indicate spin-locking is not taking place. The τ spacing in the experiment was set to 10 μs, the $\pi/2$ pulse was 1.5 μs and the phase shift was set to 45°. The resulting line-narrowing was ~27 Hz. The insets above shows the FID for the same sequence without the phase toggle, and that below the dependence of line-narrowing as a function of offset.

short τ spacings. For both the SME2 and SME8 cycles it was also found that the line-narrowing improved as the off-resonance condition was increased, probably due to a second averaging effect [31].

Though the assumption $2\omega_{RF}\tau = (2n+1)\pi,\ n \in Z$ was imposed for our sequences to be symmetric, the effect of this criterion could not be experimentally observed in any of the cycles. This may indicate that at the applied RF field strengths, higher order terms of the Magnus expansion are being suppressed to the extent that the spin dynamics are not greatly affected by these contributions. An additional argument may be made

that errors such as phase transients dominate the spin evolution and suppress the extent to which the symmetry condition may be experimentally observed.

In a rigid solid such as single crystal calcium fluoride, the interaction of the nuclear spin system with sparse paramagnetic impurities results in an irreversible spin evolution which cannot be refocused by a ME pulse. The T_1 relaxation of the sample provides a measure of the extent to which the system evolves irreversibly, and the lower limit to the linewidth is $1/\pi T_1$. For the sample studied, the T_1 was on the order of 10 s, which corresponds to a spectrum linewidth of approximately 0.03 Hz. The practical limits of resolution are still limited by instrumental imperfections and modulation schemes.

4. Conclusions

Average Hamiltonian techniques, familiar in multiple pulse NMR experiments, were applied to the ME sequence to correct for finite pulse width effects and other pulse errors. The pulse sequences developed by these methods were applied to a single crystal of calcium fluoride and resulted in efficient line-narrowing. By proper application of gradient pulses during the free evolution times these sequence may also be applied to imaging or diffusion experiments and are expected to improve the resolution and sensitivity in each of these fields, respectively.

Acknowledgments

We thank J.S. Waugh, E.M. Fortunato, and M.A. Pravia for useful discussions. The research was supported by the NSF and DARPA

References

[1] U. Haeberlen, J.S. Waugh, Coherent averaging effects in magnetic resonance, Phys. Rev. 175 (1968) 453–467.
[2] P. Mansfield, M.J. Orchard, D.C. Stalker, K.H.B. Richards, Symmetrized multipulse nuclear-magnetic-resonance experiments in solids: measurement of the chemical-shift shielding tensor in some compounds, Phys. Rev. B 7 (1973) 90–105.
[3] W.-K. Rhim, D.D. Elleman, R.W. Vaugan, Enhanced resolution for solid-state NMR, J. Chem. Phys. 58 (1973) 1772–1773.
[4] J.S. Waugh, L.M. Huber, U. Haeberlen, Approach to high-resolution NMR in solids, Phys. Rev. Lett. 20 (1968) 180–182.
[5] K. Takegoshi, C.A. McDowell, A magic echo pulse sequence for the high-resolution NMR spectra of abundant spins in solids, Chem. Phys. Lett. 116 (1985) 100–104.
[6] S. Matsui, Suppressing the zero-frequency artifact in magic-sandwich-echo proton images of solids, J. Magn. Reson. 98 (1992) 618–621.
[7] W.-K. Rhim, A. Pines, J.S. Waugh, Time-reversal experiments in dipolar-coupled spin systems, Phys. Rev. B 3 (1971) 684–696.
[8] S. Matsui, Solid-state NMR imaging by magic sandwich echoes, Chem. Phys. Lett. 179 (1991) 187–190.
[9] U. Haeberlen, High Resolution NMR in Solids: Selective Averaging, Academic Press, New York, 1976.
[10] M. Matti Maricq, Application of average Hamiltonian theory to the NMR of solids, Phys. Rev. B 25 (1982) 6622–6632.
[11] S. Matsui, Y. Ogasawara, T. Inouye, Proton images of elastomers by solid-state NMR imaging, J. Magn. Reson. A 105 (1993) 215–218.
[12] S. Matsui, A. Uraoka, T. Inouye, Improved resolution in solid-state NMR imaging by self-phase encoding, J. Magn. Reson. A 112 (1995) 130–133.
[13] S. Matsui, A. Uraoka, T. Inouye, Solid-state NMR imaging by tetrahedral-magic-echo time-suspension sequences, J. Magn. Reson. A 120 (1996) 11–17.
[14] S. Matsui, S. Saito, Symmetric echo acquisition for absolute-value display in solid-state NMR imaging, J. Magn. Reson. 149 (2001) 103–109.
[15] M.A. Hepp, J.B. Miller, Mapping molecular-orientation by solid-state NMR imaging, J. Magn. Reson. A 111 (1994) 62–69.
[16] W. Zhang, D.G. Cory, First direct measurement of the spin diffusion rate in a homogenous solid, Phys. Rev. Lett. 80 (1998) 1324–1327.
[17] C.H. Wang, J.D. Ramshaw, Decay of multiple spin echoes in dipolar solids, Phys. Rev. B. 6 (1972) 3253–3262.
[18] D.P. Burum, W.K. Rhim, Analysis of multiple pulse NMR in solids. III, J. Chem. Phys. 71 (1979) 944–956.
[19] D.P. Burum, M. Linder, R.R. Ernst, A new "Tune-Up" NMR pulse cycle for minimizing and characterizing phase transients, J. Magn. Reson. 43 (1981) 463–471.
[20] B.C. Gerstein, C.R. Dybowski, Transient Techniques in NMR of Solids, Academic Press, New York, 1985.
[21] S. Idziak, U. Haeberlen, Design and construction of a high homogeneity RF coil for solid-state multiple-pulse NMR, J. Magn. Reson. 50 (1982) 281–288.
[22] M. Levitt, R. Freeman, T. Frenkiel, Supercycles for broadband heteronuclear decoupling, J. Magn. Reson. 50 (1982) 157–160.
[23] A.J. Shaka, J. Keeler, R. Freeman, Evaluation of a new broadband decoupling sequence—WALTZ-16, J. Magn. Reson. 53 (1983) 313–340.
[24] J.S. Waugh, Theory of broad-band spin decoupling, J. Magn. Reson. 50 (1982) 30–49.
[25] M. Levitt, R. Freeman, T. Frenkiel, Broad-band heteronuclear decoupling, J. Magn. Reson. 47 (1982) 328–330.
[26] J.S. Waugh, Systematic procedure for constructing broad-band decoupling sequences, J. Magn. Reson. 49 (1982) 517–521.
[27] S. Matsui, H. Muira, H-1-C-13 cross-polarization using a modified magic echo sequence for H-1 spin locking, Chem. Phys. Lett. 242 (1995) 163–168.
[28] M. Hohwy, N.C. Nielson, High-order truncation in multiple pulse NMR, J. Chem. Phys. 106 (1997) 7571–7586.
[29] M.S. Conradi, A.N. Garroway, D.G. Cory, J.B. Miller, Generation of short, intense gradient pulses, J. Magn. Reson. 94 (1991) 370–375.
[30] D.G. Cory, Solid state NMR imaging, Ann. Rep. NMR Spect. 24 (1992) 87–180.
[31] A. Pines, J.S. Waugh, Quantitative aspects of coherent averaging. simple treatment of resonance offset processes in multiple-pulse NMR, J. Magn. Reson. 8 (1972) 354–365.